HHS Public Access

Author manuscript

J Proteome Res. Author manuscript; available in PMC 2018 August 04.

Published in final edited form as:

J Proteome Res. 2017 August 04; 16(8): 2825–2835. doi:10.1021/acs.jproteome.7b00140.

Global Phosphoproteomic Analysis of Insulin/Akt/mTORC1/S6K Signaling in Rat Hepatocytes

Yuanyuan Zhang[1], **Yajie Zhang**[2], and **Yonghao Yu**[2,*]

[1]Department of Molecular Genetics, University of Texas Southwestern Medical Center, Dallas, TX 75390

[2]Department of Biochemistry, University of Texas Southwestern Medical Center, Dallas, TX 75390

Abstract

Insulin resistance is a hallmark of type 2 diabetes. Although multiple genetic and physiological factors interact to cause insulin resistance, deregulated signaling by phosphorylation is a common underlying mechanism. In particular, the specific phosphorylation-dependent regulatory mechanisms and signaling outputs of insulin is poorly understood in hepatocytes, which represents one of the most important insulin-responsive cell types. Using primary rat hepatocytes as a model system, we performed reductive di-methylation (ReDi)-based quantitative mass spectrometric analysis, and characterized the phosphoproteome that is regulated by insulin, as well as its key downstream kinases including Akt, mTORC1 and S6K. We identified a total of 12,294 unique, confidently localized phosphorylation sites and 3,805 phosphorylated proteins in this single cell type. Detailed bioinformatic analysis on each individual dataset identified both known and previously unrecognized targets of this key insulin downstream effector pathway. Furthermore, integrated analysis of the hepatic Akt/mTORC1/S6K signaling axis allowed the delineation of the substrate specificity of several close-related kinases within the insulin signaling pathway. We expect that the datasets will serve as an invaluable resource, providing the foundation for future hypothesis-driven research that helps delineate the molecular mechanisms that underlie the pathogenesis of type 2 diabetes and related metabolic syndrome.

Graphical abstract

*To whom correspondence should be addressed to: Yonghao.Yu@UTSouthwestern.edu, Telephone: 214-648-3535.

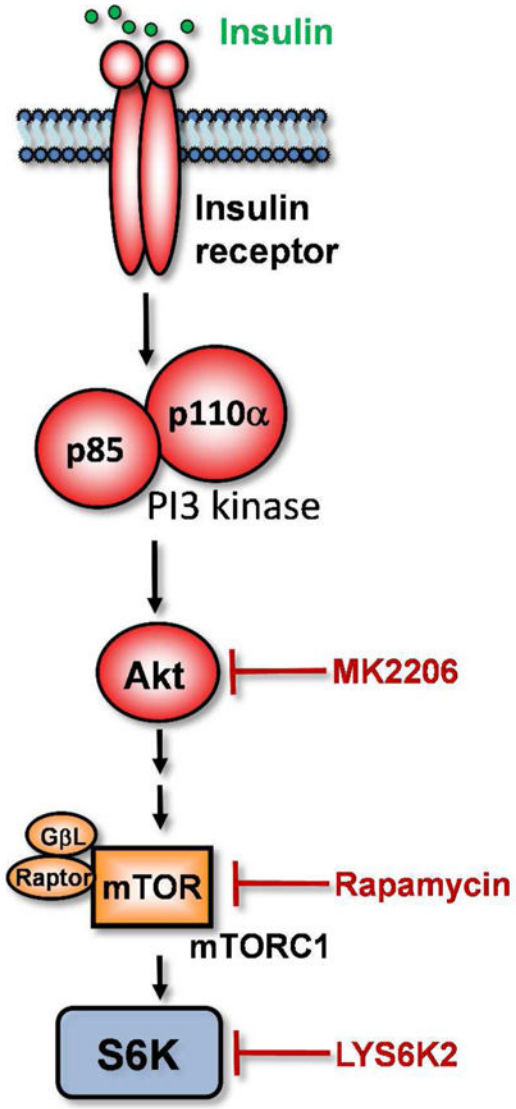

Keywords

Proteomics; phosphoproteomics; quantification; kinase; signaling; insulin; mTOR; diabetes; liver; insulin resistance

Introduction

Phosphorylation is a critical mediator of insulin-stimulated signaling pathways. Indeed, many key players in the pathway, including insulin receptor, insulin receptor substrate 1 and 2, Akt and mTORC1, are either kinase themselves and/or phosphorylated upon insulin stimulation[1, 2]. Many of these phosphorylation events further modulate their corresponding biological activity, relaying the step-wise downstream signaling to coordinate many functions of insulin. Aberrant regulation of this pathway contributes to the pathogenesis of

many human diseases, including metabolic syndrome and cancer[2]. In particular, a hallmark of type 2 diabetes is coexistence of insulin resistance and sensitivity in the liver[3]. Elevated insulin no longer suppresses glucose production, but it continues to stimulate fatty acid synthesis. This simultaneous overproduction of glucose and fatty acids in liver creates a vicious cycle that exacerbates hyperglycemia and hypertriglyceridemia[3]. Recent studies revealed that a key factor in diabetic hypertriglyceridemia is the insulin-mediated activation of sterol regulatory element-binding protein 1c (SREBP-1c), a transcriptional regulator of fatty acid synthesis that functions downstream mTORC1[4, 5]. However, due to its highly complex nature, the molecular mechanism by which mTORC1/S6K regulates the activation of SREBP-1c, and how this contributes to the paradoxical diabetic hypertriglyceridemia is still incompletely understood.

The method of choice for global identification and quantification of the (phospho)proteome is to use mass spectrometry-based quantitative proteomic approaches[6]. Because many phosphorylation events are of low abundance[7], it is imperative to perform enrichment procedures, in order to isolate phosphopeptides for reliable downstream analysis. Indeed, using orthogonal HPLC (high-performance liquid chromatography) separation techniques combined with metal ion (e.g. IMAC and TiO_2)-based affinity enrichment, a number of studies have achieved vastly improved coverage of the phosphoproteome (i.e. thousands of phosphorylation sites identified from one single organism, tissue and cell line)[8–10]. Coupled with the use of stable isotope labeling by amino acids in cell culture (SILAC), this approach also allows the quantitative comparison of the phosphoproteome in multiple biological states. For example, several groups have used large-scale quantitative mass spectrometry experiments to comprehensively characterize the proteome and phosphoproteome regulated by insulin, as well as by its downstream kinases (e.g. mTORC1)[11–18]. However, insulin-signaling pathways are known to differ in various cell types[16]. In particular, liver is one of the most important insulin-responsive organs. How activation of insulin signaling reshapes its downstream phosphoproteome in hepatocytes, however, is incompletely understood.

Although it is an invaluable tool in the field, the SILAC approach has several major limitations, one of which is the requirement of the introduction of stable isotopes in cell culture. Even though stable isotopes can also be fed to live mice to generate the SILAC animal, because a large amount of heavy amino acids (e.g. C^{13}-labeled Lys) is required for complete labeling, these experiments often become cost-prohibitive. To tackle these challenges, several methods have been developed to introduce stable isotopes at the peptide level using chemical modification (i.e. post-digestion labeling). For example, reductive dimethylation (ReDi) can reliably conjugate primary amine groups with either heavy or light labeled CH_3- group and is applicable to virtually any samples[19]. Recently, this method has been further improved, which was deployed to quantitatively compare the phosphoproteome in fasted and re-fed mouse liver[20]. In this study, Wilson-Grady et al. were able to identify hundreds of phosphorylation sites in mouse liver that differ between the fasted and refed states. Subsequently, this method was also deployed in breast cancer stem cells[21] and formalin-fixed, paraffin-embedded clear cell renal carcinoma tissue[22]. Reductive dimethylation is thus proven to be more versatile while offers similar multiplexing capabilities and quantitative accuracy as SILAC[23].

In the current study, we have focused on insulin signaling in primary rat hepatocytes, which demonstrate robust responses to insulin in vitro[24]. The preeminent consequence of insulin stimulation is the activation of a number of kinase-mediated signal transduction networks, in particular the PI3K-Akt-mTORC1-S6K pathway. Because these primary rat hepatocytes do not proliferate in culture, we used ReDi-based quantitative phosphoproteomics experiments to systematically characterize the insulin-regulated phosphoproteome in rat hepatocytes, and the subset that is sensitive to inhibitors of Akt, mTORC1 or S6K. In so doing, we mapped, in a stepwise fashion, the insulin-mediated, phosphorylation-dependent signal transduction network in hepatocytes, presenting a rich source of pathway regulators and targets for future investigation.

Materials and Methods

Materials

We obtained powdered bovine insulin from Sigma (catalog no. I6634) and protein kinase inhibitors from sources as previously described[5]. LYS6K2, obtained from Eli Lilly and Company, is a highly selective ATP inhibitor of P70 S6K[5]. A stock solution of 0.1 mM insulin was prepared by dissolving the powder in 1% (vol/vol) acetic acid, after which the solution was sterilized by filtration, and was stored in multiple aliquots at −80 °C. A working solution was made from the stock solution with the addition of sterilized acetic solution and was used immediately for experiments. All kinase inhibitors were prepared in dimethyl sulfoxide and stored at −20 °C. Culture media, FCS, and collagen-coated dishes were obtained from sources as described[24].

Primary Rat Hepatocytes

Primary hepatocytes were isolated from nonfasted rats (male, 2–3 mo old) and cultured as previously described[24]. Unless noted otherwise, on day 1, cells were pretreated for 2 h with a direct addition of 10 μL dimethyl sulfoxide with or without the indicated protein kinase inhibitor: 10 μM Akt 1/2, 0.1 μM rapamycin, or 3 μM LYS6K2. After this pre-incubation, the cells were treated with a direct addition of 10 μL acidified water with or without 100 nM insulin for 30 min, harvested in buffer containing 8 M urea, 20 mM HEPES pH 7.0, 1/500 benzonase, and then pooled (10 dishes of cells per sample). An aliquot of the samples were subjected to immunoblot and the remainders were frozen in liquid nitrogen and stored in −80 °C freezer.

Immunoblot Analysis

Aliquots were measured for protein concentration by the BCA Protein Assay kit (Pierce). Protein samples were diluted to the same concentration after the addition of 4× SDS loading buffer [0.15 mM Tris•HCl (pH 6.8), 12% (wt/vol) SDS, 0.02% (wt/vol) bromophenol blue, 30% (vol/vol) glycerol, and 6% (vol/vol) β-mercaptoethanol]. The samples then were heated at 37 °C for 1 hour and subjected to 12% SDS/PAGE. The following antibodies were used: Akt (1:2,000) (9272; Cell Signaling); phospho-Ser473-Akt (1:2,000) (4060; Cell Signaling); ribosomal protein S6 (1:2,000) (2217; Cell Signaling); and phospho-Ser235/236-ribosomal protein S6 (1:2,000) (2211; Cell Signaling).

Sample preparation for mass spectrometric analysis

Cells were lysed in urea buffer (8 M urea, 20 mM HEPES pH 7.0, 1/500 benzonase) and the lysates were reduced by adding DTT to a final concentration of 3 mM, followed by incubation at room temperature for 20 min. Cysteines were alkylated by adding iodoacetamide to a final concentration of 30 mM, followed by incubation in the dark for 20 min. The lysates were diluted to a final concentration of 2 M urea by addition of 100 mM NH_4OAC (pH 6.8) and were digested overnight with sequencing-grade trypsin (Promega) at a 1:100 (enzyme:substrate) ratio.

Digestion was quenched by addition of trifluoroacetic acid to a final concentration of 0.1% and precipitates were removed by centrifugation at 7,000 rpm for 10 min. Peptides were desalted on Oasis HLB columns (Waters): the cartridges were washed with 2 ml methanol, followed by 2 ml 0.1% TFA. Peptides were loaded and were washed with 6 ml 0.1% TFA for 4 times and were eluted with 0.1% formic acid in 40% acetonitrile. Peptides were lyophilized in a vacuum concentrator.

For reductive-dimethylation labeling experiments[20], peptides were resuspended in 1 M MES (pH 5.5) and were reacted with the light (d0-formaldehyde, $NaCNBH_3$) and heavy (d2-formaldehyde and $NaCNBD_3$) reagents, respectively, for 10 min at room temperature. The reaction was repeated once. Excessive reagents were quenched and the light and heavy peptides were combined at a 1:1 ratio. The peptides were desalted on Oasis HLB cartridges and were lyophilized.

Peptides were fractionated by strong cation exchange chromatography (SCX-HPLC)[11]. Briefly, lyophilized peptides were resuspended in 500 μl SCX buffer A (5 mM KH_2PO_4, pH 2.65, 30% acetonitrile) and injected onto a SCX column (Polysulfoethyl aspartamide, 9.4 mm×200mm, 5μmM particle size, 200 Å pore size, PolyLC). Gradient was developed over 35 min ranging from 0% to 21% buffer B (5 mM KH_2PO_4, pH 2.65, 30% acetonitrile, 350 mM KCl) at a flow rate of 3.5 ml/min. Eighteen fractions were manually collected and were lyophilized, which were subsequently desalted using Oasis HLB columns and were lyophilized.

Phosphopeptides were enriched by TiO_2 chromatography[25]. Briefly, peptides were resuspended in 50% acetonitrile containing 2 M lactic acid. Approximately 3 mg of TiO_2 beads were added to each fraction and were vortexed for 2 hrs at room temperature. The beads were washed twice with 200 μl binding solution and then washed three times with 200 μl 50/50 ACN/water, 0.1% TFA. Phosphopeptides were eluted twice by 70 μl of 50 mM KH_2PO_4 (pH adjusted to 10 using NH_4OH). The eluates were combined and the peptides were subsequently desalted by stage tips.

Mass spectrometry analysis and data processing

Samples were analyzed by LC-MS/MS on an LTQ Velos Pro Orbitrap mass spectrometer (Thermo, San Jose, CA) using a top twenty method[15]. MS/MS spectra were searched against a composite database of the rat IPI protein database (Version 3.60) and its reversed complement using the Sequest algorithm. Search results were filtered to include <1% matches to the reverse data base by the linear discriminator function using parameters

including Xcorr, dCN, missed cleavage, charge state (exclude 1+ peptides), mass accuracy, peptide length and fraction of ions matched to MS/MS spectra. Phosphorylation site localization was assessed by the ModScore algorithm[6] based on the observation of phosphorylation-specific fragment ions. Phosphorylation sites with a Modscore of at least 13 ($P \leq 0.05$) were considered to be confidently localized. Peptide quantification was performed by using the CoreQuant algorithm based on integrated peak area of precursor ions[15].

Results

A primary rat hepatocyte system for the study of insulin signaling

Many aspects of the molecular mechanisms of insulin signaling in liver remains poorly understood, in part due to the lack of a suitable in vitro biological system. Specifically, none of the established hepatocyte cell lines responds to insulin with the robustness observed in the livers of living animals, and virtually all previous studies of insulin action have been carried out in non-hepatic cell lines. For this reason, in the current study we have focused on insulin signaling in primary rat hepatocytes, which was shown recently to demonstrate robust responses to insulin in vitro[24]. It is important to note that although both mouse and rat livers respond to insulin robustly in vivo, primary mouse hepatocytes show much less sensitivity to insulin than rat hepatocytes[24]. Although numerous studies have dealt with insulin signaling in various tissues[26], only a few have been carried out in primary rat hepatocytes[5, 24, 27–32]. This system is also advantageous for the following reasons: first, we performed experiments on primary rat hepatocytes within 48 h of their isolation (primary hepatocytes lose their insulin responsiveness after 72 h); second, this system allows the study of action of insulin without the influence from other hormonal and physiological changes that occur during the refeeding process in live animals; lastly, this system is particularly amenable to pharmacological inhibitor treatment (Figure S1), which potentially allows one to not only validate phosphorylation sites identified by insulin-stimulation but also elucidate the function of new substrates and mediators in this pathway.

Generation of a large insulin-regulated phosphorylation repertoire in hepatocytes by MS

Given that phosphorylation is a transient process, we first performed a time course of insulin-stimulated Akt and S6 phosphorylation (Figure S2A.) Hepatocytes were prepared and plated on day 0 as described in Materials and Methods. On day 1, the cells were left untreated or treated with 100 nM insulin for the indicated times, harvested, and then pooled for immunoblot analysis of total- and phospho-Akt and S6. As shown in Figure S2A, when cells were exposed to 100 nM insulin, phosphorylation of Akt (S473) reached maximum in as soon as 5 minute and remained elevated until 30 minute before the level of phosphorylation went down; whereas phosphorylation of S6 (S235/236) began around 5 minute and increased to maximum at 30 minute after insulin. Therefore, we choose a brief, 30-minute insulin stimulation to capture cellular phosphorylation state under insulin stimulation with either no inhibitors or inhibitors to Akt, mTORC1 or S6K.

Because rat hepatocytes do not proliferate in culture, we utilized ReDi labeling that introduces stable isotopes post-digestion at the peptide level. We performed 4 quantitative phosphoproteomic analyses: In the first experiment, we compared starved primary

hepatocytes that were subsequently treated with or without 30 min, 100 nM insulin. This allows us to identify the proteins whose phosphorylation is stimulated by insulin. In the second experiment, we pretreated primary hepatocytes with or without MK2206 (a specific, potent inhibitor of Akt)[33], and then stimulated both group with insulin to identify insulin effector proteins whose phosphorylation is sensitive to Akt inhibition. Similarly, in the third experiment, we pretreated hepatocytes with rapamycin (mTORC1 inhibitor)[11] prior to insulin stimulation. For completion of analysis, we also added a fourth pair of comparison using an inhibitor to S6K (LYS6K2, a specific S6K inhibitor and gift from Eli Lily)[24], a critical insulin pathway kinase downstream of mTORC1. The points of inhibition are illustrated in Figure S1A and S1B.

In each set of phosphoproteomic analysis, samples were lysed, tryptic-digested, desalted and then labeled by using the reductive dimethylation reaction. In this method, all primary amines (the N terminus and the side chain of lysine residues) in a peptide mixture were converted to dimethylamines by reacting with the either light (d0-formaldehyde and $NaCNBH_3$) or heavy (d2-formaldehyde and $NaCNBD_3$) reagents using the lower pH protocol[20] (Figure S1C and Figure S2B).

Qualitative evaluation of the insulin-regulated phosphoproteome in hepatocytes

From the 4 ReDi quantitative phospho-proteomic analyses, we were able to acquire a total of 2,204,898 MS2 spectra (peptide sequencing events) (Figure S1D). MS/MS spectra were searched against a composite database of the rat IPI protein database and its reversed complement using the Sequest algorithm. They were then processed by post-search filtering, phosphorylation site assignment and quantification. We performed a detailed evaluation of the quality of the datasets. Consistent with a recent study[20], we found that lower pH ReDi is an excellent strategy that introduces stable isotope labels without affecting the properties of the phosphopeptides. Specifically, di-methylated peptides generated very similar SCX elution profiles, compared with those from other published phosphoproteomic studies[11]. Our phosphopeptide enrichment was highly efficient. For example, in the Akt-i screen, the first three SCX fractions contained more than 95% phosphopeptides, and many of them were multiply phosphorylated (Figure 1A and 1B). This is a particularly important observation because these multiply phosphorylated peptides significantly increase the final number of unique phosphorylation sites identified.

From the four screens, we were able to identify a total of 272,948 phosphopeptides (FDR = 0.18%) from 3,805 phosphoproteins. These phosphoproteins are distributed within a wide variety of cellular compartments, including cytosol, nucleoplasm, cytoskeleton, etc (Figure S3). In total, we were able to identify 12,294 unique, confidently localized (Modscore ≥ 13, or $p \leq 0.05$) phosphorylation sites (Supplementary Table 1). The majority of the phosphorylation sites (10,027 or 81.6%) are on Ser residues, while Thr and Tyr comprise of 1,879 (15.3%) and 388 (3.2%) of the phosphorylation sites, respectively (Figure 1C). We identified several highly enriched motifs around the identified phosphorylation residues, including those for Tyr (e.g. DxxY, YxD and YxxxxxS, etc.), and for Ser (e.g. PxSP, SDDE and RxxSPxP, etc.) (Figure 1E and 1F).

We identified many phosphorylation sites on proteins that are known to be involved in insulin signaling. As an example, we identified a total of 35 phosphorylation sites on IRS2 (Supplementary Table 2). Several of these sites (Figure 1D) have been shown to be critically related to the function of IRS2 in controlling cellular processes downstream of insulin[34]. Specifically, we identified three Tyr phosphorylation sites on IRS2 (Tyr650, Tyr672 and Tyr735), all of which are located within a YMxM motif. Intriguingly, phosphotyrosine in this motif is known to mediate the binding to the p85 regulatory subunit, and thus recruitment of PI3 kinase[35]. Indeed, a recent study demonstrated that mutation of either Tyr650 or Tyr672 greatly reduced the overall tyrosine phosphorylation of IRS2. Importantly, these phosphotyrosine residues (Tyr650, Tyr672 and Tyr735) are essential for the initiation of several critical molecular events upon insulin stimulation, including the association of IRS2 with PI3K, Akt activation and glucose uptake[34].

Quantitative phosphoproteomic analyses of the insulin/Akt/mTORC1/S6K network in hepatocytes

Next we performed a series of quantitative evaluation of the data from the four ReDi screens (Supplementary Tables 3–6). In the first set of analysis, peptides from serum starved hepatocytes without insulin stimulation were labeled with light isotopes while the insulin-stimulated samples were labeled with heavy isotopes (Figure S1D). In this analysis, we acquired a total of 409,563 MS2 spectra. Using a 1% FDR (protein level) as the filtering threshold, we were able to identify a total of 37,366 phosphopeptides. Over 90% of the identified phosphopeptides were present in equal amounts between heavy and light labeled samples, therefore clustering around zero on a Log_2(insulin/control) scale (Figure S4 and Supplementary Table 3). Phosphopeptides with a positive Log_2H/L are those whose phosphorylation levels are increased by insulin stimulation (circled in red). We identified 1,361 phosphopeptides from 210 proteins whose phosphorylation is increased by at least 2-fold upon insulin stimulation (Figure S4). Manual inspection revealed that this list of proteins contains many known players in the insulin pathway, including: IRS1/2, Raptor, Acly, FoxK1, Eif4ebp, Lpin1, GSK3 and Grb10, etc. Indeed, Gene Ontology analysis showed that these 210 proteins are highly enriched with proteins involved in biological processes that are connected to insulin signaling, including cellular response to insulin stimulus ($P = 1.34 \times 10^{-8}$), insulin receptor signaling pathway ($P = 2.64 \times 10^{-5}$), positive regulation of glucose metabolic process ($P = 6.45 \times 10^{-5}$), etc (Figure S4). For the insulin screen, we also performed a biological replicate experiment. From this analysis, we were able to identify 41,888 phosphopeptides (using 1% protein FDR) from a total of 407,577 MS2 sequencing events. Similarly, using a 2-fold increase in the abundance of a corresponding phosphopeptide as the threshold, we identified many known insulin downstream effector proteins, including IRS1/2, Acly, FoxK1, NDRG1/2, GSK3, Grb10, etc.

In the second set of analysis, we compared insulin-stimulated samples in the presence and absence of pre-treatment of an Akt1/2 inhibitor, MK2206 (Supplementary Table 4). The distribution of Log_2H/L is plotted in Figure 2A, again showing that the vast majority of the peptides have equal amounts between MK2206-treated sample, and the control sample. Using a cutoff of 2-fold (phosphorylation decreased by 2-fold or more in MK2206-treated

sample, compared to control), we identified 2,033 phosphopeptides, which corresponded to 545 proteins. Gene ontology analysis of the decreased proteins shows that they are enriched with a number of Akt-related biological processes, including regulation of Ras protein signal transduction ($P = 3.04 \times 10^{-8}$), mRNA processing ($P = 4.3 \times 10^{-7}$) and regulation of phosphate metabolic process ($P = 4.38 \times 10^{-7}$), etc (Figure 2B). This extensive list includes many known Akt downstream targets, including IRS1/2, Akt1s1, Eif4ebp, Lpin, ULK1/2, Tfeb, Depdc6, Raptor and Rictor, etc. Other known proteins in the pathway include Gab1 and Grb7. As an example, we identified a phosphopeptide from IRS2 (TDS*LAAT*PPAAK, the asterisks indicate the sites of phosphorylation at Ser344 and Thr348). This phosphopeptide showed strong sensitivity to Akt inhibition, the abundance of which decreased by more than 7-fold after MK2206 treatment (Figure 2C and 2D). We also identified a number of phosphorylation sites from ribosomal protein S6, including a doubly phosphorylated peptide (LS*SLRAS*TSK, the asterisks indicate the sites of phosphorylation at Ser235 and Ser240). Interestingly, the phosphorylation of these two Ser residues (correspond to Ser235 and Ser240 in the human protein) showed little change after Akt inhibitor treatment (Figure 2E and 2F), an observation that is consistent with that from independent immunoblotting experiments performed in these hepatocytes (Figure S1B).

In the third analysis, we compared insulin-stimulated samples in the presence and absence of rapamycin pre-treatment (Supplementary Table 5). Again the vast majority of the phosphopeptides have equal amounts between rapamycin-treated sample, and the control sample (Figure 3A). We identified 954 phosphopeptides from 323 proteins whose phosphorylation decreased by 2-fold or more in rapamycin-treated sample, compared to control. Gene ontology analysis of the decreased proteins shows that they are enriched with mTORC1-relevant biological processes including regulation of mRNA processing ($P = 1.32 \times 10^{-7}$), regulation of transcription ($P = 3.09 \times 10^{-7}$) and positive regulation of macromolecule metabolic process ($P = 1.77 \times 10^{-6}$), etc (Figure 3B). This list includes many known mTORC1 downstream targets, including IRS1/2, rpS6, Eif4ebp, PDCD4, Lpin1, ULK1/2, Tfeb, Depdc6 and Rictor, etc. For example, in the rapamycin screen, we identified a phosphopeptide from IRS2 (SRTDS*LAAT*PPAAK) that contains the same phosphorylation sites as those in the peptide identified in the Akt-inhibitor screen. In this case, this IRS2 phosphopeptide also showed sensitivity to mTORC1 inhibition, with its abundance decreased by about 3-fold after rapamycin treatment (Figure 3C and 3D). Intriguingly, Ser344 and its preceding amino acid sequence (i.e. RSRTDS*) are located within in an amino acid sequence of RxRxxS/T (Arg at the -3 and -5 positions relative to the phosphorylated Ser or Thr), a substrate motif that is shared by a number of basophilic kinases, including Akt and S6K[36, 37]. These data suggest that IRS2 phosphorylation at Ser344 could be mediated by Akt and/or its more downstream target S6K. Similarly, we also identified the doubly phosphorylated peptide from rpS6 (LS*SLRAS*TSK, the asterisks indicate that sites of phosphorylation at Ser235 and Ser240). The phosphorylation of these two Ser residues decreased by more than 50-fold after rapamycin treatment, which is consistent with it being a substrate of S6K (Figure 3E and F).

In the fourth analysis, we compared insulin-stimulated samples in the presence and absence of the pre-treatment of an S6K inhibitor, LYS6K2 (Supplementary Table 6). From this screen, we were able to identify a total of 59,457 phosphopeptides. Using a cutoff of 2-fold

(phosphorylation decreased by 2-fold or more in LYS6K2-treated sample, compared to control), we identified 868 phosphopeptides, which corresponded to 318 proteins (Figure S5A). This list includes many known S6K downstream targets, including IRS2, eIF4B, rpS6 and PDCD4, etc. Gene ontology analysis of the decreased proteins (proteins with decreased phosphorylation after LYS6K2 treatment) shows that they are enriched with biological processes including regulation of regulation of Ras protein signal transduction ($P = 2.44 \times 10^{-6}$), regulation of cellular ketone metabolic process ($P = 8.7 \times 10^{-4}$) and posttranscriptional regulation of gene expression ($P = 0.001$), etc (Figure S5B).

Integrated analyses of the phosphoproteome regulated by the insulin/Akt/mTORC1/S6K pathway in hepatocytes

The PI3K/Akt/mTORC1 pathway regulates a diverse array of biological processes, many of which are connected to the cellular effects of insulin. Our dataset provides an opportunity to systematically interrogate the insulin-regulated phosphoproteome in hepatocytes in a step-wise fashion. We performed cross-reference analysis of the results from the insulin screen and Akt-i screen. In this case, we extracted the phosphopeptides that were commonly identified in these two experiments, and plotted their level of changes in their corresponding treatment conditions (Figure 4A). We are particularly interested in the phosphopeptides (those in the highlighted area in Figure 4A) whose abundances increased by more than 2-fold upon insulin stimulation (derived from the insulin screen), but decreased by more than 2-fold upon MK2206 pre-treatment in the Akt-i screen. These proteins, along with their phosphorylation sites, represent particularly good candidates as potential targets regulated by Akt. As an example, we found that the level of a phosphopeptide (LFS*QGQDVSDK) from Mllt4 (also known as Afadin) increased by more than 20-fold upon insulin treatment. The same phosphopeptide, however, decreased by about 7-fold upon the pre-treatment of hepatocytes with MK2206 (Figure 4A). Afadin is known to be localized at the leading edge of moving cells, and is involved in regulating growth factor-dependent, directional cell movement[38–40]. Intriguingly, this site (S1804, which corresponds to S1795 in the mouse protein) is within the AGC consensus motif (RxRxxS/T), and it was reported to be an insulin-responsive phosphorylation site in a quantitative phosphoproteomic study of the mouse liver[18]. Furthermore, this site was recently shown to be directly modified by Akt in breast cancer cells, and this phosphorylation event promotes the nuclear localization of Afadin, and increases breast cancer cell migration[40]. Other proteins with similar patterns of change (i.e. increased in insulin screen, and decreased in Akt-i screen) include Akt1s1 (LNT*SDFQK), which has been previously suggested to function downstream of Akt[41].

Next we similarly extracted the phosphopeptides commonly identified between the insulin screen and the rapamycin screen, and highlighted the ones that are potentially regulated by mTORC1 (i.e. increased by more than 2-fold in insulin screen, and decreased by more than 2-fold upon rapamycin pre-treatment) (Figure 4B). These include phosphopeptides from Larp1 (TASISSSPSEGTPAVGSYGCT*PQS*LPK) and Prkaa2 (MPPLIADS*PK). Interestingly, the rapamycin-sensitive phosphorylation sites in a number of established mTORC1 substrates are known to be localized in very different motifs (e.g. TY in S6K and S/TP in 4EBP and Grb10)[11]. Using a positional scanning peptide library, Kang et al. characterized the substrate motifs of mTORC1, and found that mTORC1 strongly prefers

S/T residues with P, hydrophobic (L and V), or aromatic residues (F, W and Y) at the +1 position[42]. Based on these results, the two aforementioned proteins therefore are more likely to be directly phosphorylated by mTORC1 rather than an mTORC1 downstream kinase (e.g. S6K). Intriguingly, Larp1 was previously shown to bear rapamycin-sensitive phosphorylation sites in other cell types[11, 12]. Moreover, Larp1 was recently demonstrated to play a critical role in regulating protein synthesis[43]. Specifically, Larp1 binds to the mRNA 5′ cap in an mTORC1-dependent manner. In so doing, Larp1 stimulates the translation of mRNA that contain a 5′ terminal oligopyrimidine (TOP), a motif found in transcripts whose translation is specifically regulated by mTORC1[44]. We, at the same time, also observed a number of phosphopeptides, in particular those clustered on/around the X-axis, whose phosphorylation is positively regulated by insulin, but is not affected by rapamycin treatment. They could potentially be modified by an insulin-dependent kinase that, however, functions upstream of and/or in parallel with mTORC1 (Figure 4B).

Through cross-reference analysis between the insulin screen and S6K-i screen, we identified a number of insulin downstream effector proteins whose phosphorylation is regulated by S6K (i.e. increased by more than 2-fold in insulin screen, and decreased by more than 2-fold upon LYS6K2 pre-treatment) (Figure 4C). For example, the level of a phosphopeptide (IHRAS*DPGLPAEEPK) from CAD (carbamoyl-phosphate synthetase 2, aspartate transcarbamoylase, dihydroorotase, S1859, which corresponds to S1859 in the human protein) increased by 2.7-fold after insulin stimulation, while decreased by about 3-fold upon pre-treating the cells with LYS6K2. This phosphorylation residue was also identified to be an mTORC1-regulated phosphorylation site in two phosphoproteomic screens that were performed in other cell types[11, 12]. mTORC1 activation promotes metabolic flux through the de novo pyrimidine synthesis, and thus the production of nucleotides required for cell cycle progression. Intriguingly, it was shown that this effect could be largely ascribed to S6K-dependent phosphorylation at the aforementioned site, and activation of CAD, which is the enzyme that catalyzes the first three steps of de novo pyrimidine synthesis[17, 45].

Finally, we extracted the phosphopeptides that were commonly identified between the Rapa screen and S6K-i screen, and highlighted the peptides whose phosphorylation was decreased by more than 2-fold in both screens (Figure 4D). These peptides presumably represent proteins whose phosphorylation is controlled by S6K (e.g. rpS6 LS*SLRAS*TSK). At the same time, a number of phosphopeptides clustered on/around the X-axis, whose phosphorylation is decreased upon rapamycin treatment, but is not affected by LYS6K2 treatment, could potentially represent direct mTORC1 targets (Figure 4D).

Discussion

Insulin resistance is a hallmark of type 2 diabetes. Although multiple genetic and physiological factors interact to cause insulin resistance, deregulated signaling by phosphorylation is a common underlying mechanism. Indeed, many key players in the pathway, such as insulin receptor, insulin receptor substrate 1 and 2, Akt, mTORC1 and S6K, are either kinase themselves, and/or activated in a phosphorylation-dependent manner upon insulin stimulation. The phosphoproteome that is regulated by the PI3K/Akt/mTORC1 pathway has been characterized by a series of quantitative mass spectrometric studies[11–18].

Notably, the regulatory mechanisms and signaling outputs of insulin could differ in various cell types[16]. Our system has several unique advantages for understanding phosphorylation-dependent regulatory mechanisms in a key insulin-responsive cell type (i.e. liver cells). We use primary rat hepatocytes that robustly respond to insulin stimulation in vitro[24]. This system allows study of insulin's action without the influence from other hormonal and physiological changes that occur during the refeeding process. Furthermore, this system is also particularly amenable to inhibitor treatment, which greatly facilitates the further biochemical validation and functional characterization experiments.

We previously used a SILAC-based quantitative phosphoproteomic approach to characterization of the mTORC1 downstream targets in MEFs[11]. However, SILAC is limited in that it is incompatible with primary cells that do not divide in cell culture. To tackle these challenges, we used an alternative method to introduce isotopes at the peptide level by reductive dimethylation. Importantly, ReDi labeling does not affect the elution profile of phosphopeptides during HPLC separation, or their fragmentation behavior during tandem MS analysis[20].

Using the ReDi labeling strategy, we systematically characterized insulin signaling in rat hepatocytes. By utilizing inhibitors that specifically block key downstream kinases (i.e. Akt, mTORC1 and S6K), we were able to generate, in a step-wise fashion, an atlas for the phosphoproteome regulated by insulin as well as these nodal enzymes. From the four ReDi screens, we were able to acquire a total of 2,204,898 MS2 spectra, which led to the identification of 12,294 unique, confidently localized phosphorylation sites. Unlike the SILAC labeling strategy, in which carbon and nitrogen are often chosen as the stable isotopes, heavy ReDi-labeled peptides contain deuterium. This could result in a slight difference in the HPLC retention time between the light and heavy peptides (Figure 2F), knowns as the "deuterium effect"[46]. In this case, it is important to integrate the area of the ion chromatograms, rather than use maximal peak intensities, to accurately determine the heavy to light peptide ratio. Finally, it has been shown that, in MS1-based quantification methods (i.e. SILAC and ReDi), false positive hits tend to cluster in the regulated sites (the ones with large fold-of-changes)[20]. In order to control these peptides, we performed stringent data filtering at both peptide and protein levels (FDR set to be 1% for both). This step has been shown to effectively reduce the FDR for the regulated phosphorylation sites[20].

Insulin stimulation leads to the activation of downstream kinases (Figure 5), many of which share similar substrate specificity. For example, both Akt and S6K are AGC kinases that preferentially phosphorylate RxRxxS/T motifs[37, 47]. It is conceivable that, in certain conditions, the substrate protein of one AGC kinase may be recognized, and phosphorylated by another member of the AGC kinase family, a scenario that could lead to an altered signaling output. Indeed, it has been shown that GSK3β S9, a residue that is usually phosphorylated by Akt, could be directly modified by S6K in cells with hyperactive mTORC1 (e.g. *TSC2*−/− cells). This phosphorylation event leads to the inhibition of GSK3β, and its downstream signaling, which contributes to the growth factor-independent proliferation of these cells[48]. Because the four ReDi datasets were collected in one cell type (i.e. hepatocyte) under the common insulin stimulation conditions, these results facilitate the evaluation of proteins that are potentially phosphorylated by a specific insulin-regulated

kinase, or are commonly modified by multiple kinases with overlapping substrate specificity (e.g. Akt and S6K) (Figure 4). Similarly, cross-reference analysis of these datasets in a quantitative manner will also facilitate the delineation of the topological feature of the pathway.

Conclusion

In conclusion, we present here a quantitative atlas of the hepatocyte phosphoproteome that is regulated by insulin, as well as its key downstream kinases including Akt, mTORC1 and S6K. Detailed bioinformatic analysis on each individual dataset identified many biological processes that are known to be regulated upon perturbing these nodal kinases. Furthermore, the data were integrated using in silico approaches which allowed the delineation of the substrate specificity of several close-related kinases within the insulin signaling pathway. Here we have highlighted only a subset results derived from our unbiased, quantitative phosphoproteome analysis. However, we expect that the datasets contain many previously unrecognized targets of insulin signaling that will serve as an invaluable resource, seeding future hypothesis-driven research that helps dissect the complex molecular underpinnings of pathophysiological responses of the liver to insulin.

Supplementary Material

Refer to Web version on PubMed Central for supplementary material.

Acknowledgments

We thank Drs. Michael S. Brown and Joseph L. Goldstein for invaluable advice and a critical review of the paper. This work was supported in part by grants from the National Institutes of Health (NIH) (GM114160 to Y. Y.) and (HL20948 to J. L. Goldstein and M. S. Brown). Y. Y. is a Virginia Murchison Linthicum Scholar in Medical Research and a CPRIT Scholar in Cancer Research. Yuanyuan Zhang was supported by Medical Scientist Training Program Grant ST32GM08014.

References

1. Manning BD, Cantley LC. AKT/PKB signaling: navigating downstream. Cell. 2007; 129(7):1261–74. [PubMed: 17604717]
2. Zoncu R, Efeyan A, Sabatini DM. mTOR: from growth signal integration to cancer, diabetes and ageing. Nat Rev Mol Cell Biol. 2011; 12(1):21–35. [PubMed: 21157483]
3. Brown MS, Goldstein JL. Selective versus total insulin resistance: a pathogenic paradox. Cell Metab. 2008; 7(2):95–6. [PubMed: 18249166]
4. Brown MS, Goldstein JL. The SREBP pathway: regulation of cholesterol metabolism by proteolysis of a membrane-bound transcription factor. Cell. 1997; 89(3):331–40. [PubMed: 9150132]
5. Li S, Brown MS, Goldstein JL. Bifurcation of insulin signaling pathway in rat liver: mTORC1 required for stimulation of lipogenesis, but not inhibition of gluconeogenesis. Proc Natl Acad Sci U S A. 2010; 107(8):3441–6. [PubMed: 20133650]
6. Huttlin EL, Jedrychowski MP, Elias JE, Goswami T, Rad R, Beausoleil SA, Villen J, Haas W, Sowa ME, Gygi SP. A tissue-specific atlas of mouse protein phosphorylation and expression. Cell. 2010; 143(7):1174–89. [PubMed: 21183079]
7. Wu R, Haas W, Dephoure N, Huttlin EL, Zhai B, Sowa ME, Gygi SP. A large-scale method to measure absolute protein phosphorylation stoichiometries. Nat Methods. 2011; 8(8):677–83. [PubMed: 21725298]

8. Aebersold R, Mann M. Mass-spectrometric exploration of proteome structure and function. Nature. 2016; 537(7620):347–55. [PubMed: 27629641]
9. Chen IH, Xue L, Hsu CC, Paez JS, Pan L, Andaluz H, Wendt MK, Iliuk AB, Zhu JK, Tao WA. Phosphoproteins in extracellular vesicles as candidate markers for breast cancer. Proc Natl Acad Sci U S A. 2017; 114(12):3175–3180. [PubMed: 28270605]
10. Tan H, Wu Z, Wang H, Bai B, Li Y, Wang X, Zhai B, Beach TG, Peng J. Refined phosphopeptide enrichment by phosphate additive and the analysis of human brain phosphoproteome. Proteomics. 2015; 15(2–3):500–7. [PubMed: 25307156]
11. Yu Y, Yoon SO, Poulogiannis G, Yang Q, Ma XM, Villen J, Kubica N, Hoffman GR, Cantley LC, Gygi SP, Blenis J. Phosphoproteomic analysis identifies Grb10 as an mTORC1 substrate that negatively regulates insulin signaling. Science. 2011; 332(6035):1322–6. [PubMed: 21659605]
12. Hsu PP, Kang SA, Rameseder J, Zhang Y, Ottina KA, Lim D, Peterson TR, Choi Y, Gray NS, Yaffe MB, Marto JA, Sabatini DM. The mTOR-regulated phosphoproteome reveals a mechanism of mTORC1-mediated inhibition of growth factor signaling. Science. 2011; 332(6035):1317–22. [PubMed: 21659604]
13. Parker BL, Yang G, Humphrey SJ, Chaudhuri R, Ma X, Peterman S, James DE. Targeted phosphoproteomics of insulin signaling using data-independent acquisition mass spectrometry. Sci Signal. 2015; 8(380):rs6. [PubMed: 26060331]
14. Schwarz JJ, Wiese H, Tolle RC, Zarei M, Dengjel J, Warscheid B, Thedieck K. Functional Proteomics Identifies Acinus L as a Direct Insulin- and Amino Acid-Dependent Mammalian Target of Rapamycin Complex 1 (mTORC1) Substrate. Mol Cell Proteomics. 2015; 14(8):2042–55. [PubMed: 25907765]
15. Ding M, Bruick RK, Yu Y. Secreted IGFBP5 mediates mTORC1-dependent feedback inhibition of IGF-1 signalling. Nat Cell Biol. 2016; 18(3):319–27. [PubMed: 26854565]
16. Humphrey SJ, Yang G, Yang P, Fazakerley DJ, Stockli J, Yang JY, James DE. Dynamic adipocyte phosphoproteome reveals that Akt directly regulates mTORC2. Cell metabolism. 2013; 17(6): 1009–20. [PubMed: 23684622]
17. Robitaille AM, Christen S, Shimobayashi M, Cornu M, Fava LL, Moes S, Prescianotto-Baschong C, Sauer U, Jenoe P, Hall MN. Quantitative phosphoproteomics reveal mTORC1 activates de novo pyrimidine synthesis. Science. 2013; 339(6125):1320–3. [PubMed: 23429704]
18. Humphrey SJ, Azimifar SB, Mann M. High-throughput phosphoproteomics reveals in vivo insulin signaling dynamics. Nat Biotechnol. 2015; 33(9):990–5. [PubMed: 26280412]
19. Boersema PJ, Raijmakers R, Lemeer S, Mohammed S, Heck AJ. Multiplex peptide stable isotope dimethyl labeling for quantitative proteomics. Nature protocols. 2009; 4(4):484–94. [PubMed: 19300442]
20. Wilson-Grady JT, Haas W, Gygi SP. Quantitative comparison of the fasted and re-fed mouse liver phosphoproteomes using lower pH reductive dimethylation. Methods. 2013; 61(3):277–86. [PubMed: 23567750]
21. Yi T, Zhai B, Yu Y, Kiyotsugu Y, Raschle T, Etzkorn M, Seo HC, Nagiec M, Luna RE, Reinherz EL, Blenis J, Gygi SP, Wagner G. Quantitative phosphoproteomic analysis reveals system-wide signaling pathways downstream of SDF-1/CXCR4 in breast cancer stem cells. Proc Natl Acad Sci U S A. 2014; 111(21):E2182–90. [PubMed: 24782546]
22. Weisser J, Lai ZW, Bronsert P, Kuehs M, Drendel V, Timme S, Kuesters S, Jilg CA, Wellner UF, Lassmann S, Werner M, Biniossek ML, Schilling O. Quantitative proteomic analysis of formalin-fixed, paraffin-embedded clear cell renal cell carcinoma tissue using stable isotopic dimethylation of primary amines. BMC Genomics. 2015; 16:559. [PubMed: 26220445]
23. Billing AM, Ben Hamidane H, Graumann J. Quantitative proteomic approaches in mouse: stable isotope incorporation by metabolic (SILAC) or chemical labeling (reductive dimethylation) combined with high-resolution mass spectrometry. Curr Protoc Mouse Biol. 2015; 5(1):1–20. [PubMed: 25727197]
24. Owen JL, Zhang Y, Bae SH, Farooqi MS, Liang G, Hammer RE, Goldstein JL, Brown MS. Insulin stimulation of SREBP-1c processing in transgenic rat hepatocytes requires p70 S6-kinase. Proc Natl Acad Sci U S A. 2012; 109(40):16184–9. [PubMed: 22927400]

25. Erickson BK, Jedrychowski MP, McAlister GC, Everley RA, Kunz R, Gygi SP. Evaluating multiplexed quantitative phosphopeptide analysis on a hybrid quadrupole mass filter/linear ion trap/orbitrap mass spectrometer. Anal Chem. 2015; 87(2):1241–9. [PubMed: 25521595]
26. Krycer JR, Sharpe LJ, Luu W, Brown AJ. The Akt-SREBP nexus: cell signaling meets lipid metabolism. Trends Endocrinol Metab. 2010; 21(5):268–76. [PubMed: 20117946]
27. Chen G, Liang G, Ou J, Goldstein JL, Brown MS. Central role for liver X receptor in insulin-mediated activation of Srebp-1c transcription and stimulation of fatty acid synthesis in liver. Proc Natl Acad Sci U S A. 2004; 101(31):11245–50. [PubMed: 15266058]
28. Foretz M, Guichard C, Ferre P, Foufelle F. Sterol regulatory element binding protein-1c is a major mediator of insulin action on the hepatic expression of glucokinase and lipogenesis-related genes. Proc Natl Acad Sci U S A. 1999; 96(22):12737–42. [PubMed: 10535992]
29. Hegarty BD, Bobard A, Hainault I, Ferre P, Bossard P, Foufelle F. Distinct roles of insulin and liver X receptor in the induction and cleavage of sterol regulatory element-binding protein-1c. Proc Natl Acad Sci U S A. 2005; 102(3):791–6. [PubMed: 15637161]
30. Shimomura I, Bashmakov Y, Ikemoto S, Horton JD, Brown MS, Goldstein JL. Insulin selectively increases SREBP-1c mRNA in the livers of rats with streptozotocin-induced diabetes. Proc Natl Acad Sci U S A. 1999; 96(24):13656–61. [PubMed: 10570128]
31. Shimomura I, Matsuda M, Hammer RE, Bashmakov Y, Brown MS, Goldstein JL. Decreased IRS-2 and increased SREBP-1c lead to mixed insulin resistance and sensitivity in livers of lipodystrophic and ob/ob mice. Mol Cell. 2000; 6(1):77–86. [PubMed: 10949029]
32. Yellaturu CR, Deng X, Cagen LM, Wilcox HG, Park EA, Raghow R, Elam MB. Posttranslational processing of SREBP-1 in rat hepatocytes is regulated by insulin and cAMP. Biochem Biophys Res Commun. 2005; 332(1):174–80. [PubMed: 15896314]
33. Hirai H, Sootome H, Nakatsuru Y, Miyama K, Taguchi S, Tsujioka K, Ueno Y, Hatch H, Majumder PK, Pan BS, Kotani H. MK-2206, an allosteric Akt inhibitor, enhances antitumor efficacy by standard chemotherapeutic agents or molecular targeted drugs in vitro and in vivo. Mol Cancer Ther. 2010; 9(7):1956–67. [PubMed: 20571069]
34. Landis J, Shaw LM. Insulin receptor substrate 2-mediated phosphatidylinositol 3-kinase signaling selectively inhibits glycogen synthase kinase 3beta to regulate aerobic glycolysis. J Biol Chem. 2014; 289(26):18603–13. [PubMed: 24811175]
35. Songyang Z, Shoelson SE, Chaudhuri M, Gish G, Pawson T, Haser WG, King F, Roberts T, Ratnofsky S, Lechleider RJ, et al. SH2 domains recognize specific phosphopeptide sequences. Cell. 1993; 72(5):767–78. [PubMed: 7680959]
36. Yu Y, Anjum R, Kubota K, Rush J, Villen J, Gygi SP. A site-specific, multiplexed kinase activity assay using stable-isotope dilution and high-resolution mass spectrometry. Proc Natl Acad Sci U S A. 2009; 106(28):11606–11. [PubMed: 19564600]
37. Pearce LR, Komander D, Alessi DR. The nuts and bolts of AGC protein kinases. Nat Rev Mol Cell Biol. 2010; 11(1):9–22. [PubMed: 20027184]
38. Miyata M, Ogita H, Komura H, Nakata S, Okamoto R, Ozaki M, Majima T, Matsuzawa N, Kawano S, Minami A, Waseda M, Fujita N, Mizutani K, Rikitake Y, Takai Y. Localization of nectin-free afadin at the leading edge and its involvement in directional cell movement induced by platelet-derived growth factor. J Cell Sci. 2009; 122(Pt 23):4319–29. [PubMed: 19887591]
39. Miyata M, Rikitake Y, Takahashi M, Nagamatsu Y, Yamauchi Y, Ogita H, Hirata K, Takai Y. Regulation by afadin of cyclical activation and inactivation of Rap1, Rac1, and RhoA small G proteins at leading edges of moving NIH3T3 cells. J Biol Chem. 2009; 284(36):24595–609. [PubMed: 19589776]
40. Elloul S, Kedrin D, Knoblauch NW, Beck AH, Toker A. The adherens junction protein afadin is an AKT substrate that regulates breast cancer cell migration. Molecular cancer research: MCR. 2014; 12(3):464–76. [PubMed: 24269953]
41. Kovacina KS, Park GY, Bae SS, Guzzetta AW, Schaefer E, Birnbaum MJ, Roth RA. Identification of a proline-rich Akt substrate as a 14-3-3 binding partner. J Biol Chem. 2003; 278(12):10189–94. [PubMed: 12524439]

42. Kang SA, Pacold ME, Cervantes CL, Lim D, Lou HJ, Ottina K, Gray NS, Turk BE, Yaffe MB, Sabatini DM. mTORC1 phosphorylation sites encode their sensitivity to starvation and rapamycin. Science. 2013; 341(6144):1236566. [PubMed: 23888043]
43. Tcherkezian J, Cargnello M, Romeo Y, Huttlin EL, Lavoie G, Gygi SP, Roux PP. Proteomic analysis of cap-dependent translation identifies LARP1 as a key regulator of 5′ TOP mRNA translation. Genes Dev. 2014; 28(4):357–71. [PubMed: 24532714]
44. Thoreen CC, Chantranupong L, Keys HR, Wang T, Gray NS, Sabatini DM. A unifying model for mTORC1-mediated regulation of mRNA translation. Nature. 2012; 485(7396):109–13. [PubMed: 22552098]
45. Ben-Sahra I, Howell JJ, Asara JM, Manning BD. Stimulation of de novo pyrimidine synthesis by growth signaling through mTOR and S6K1. Science. 2013; 339(6125):1323–8. [PubMed: 23429703]
46. Iyer SS, Zhang ZP, Kellogg GE, Karnes HT. Evaluation of deuterium isotope effects in normal-phase LC-MS-MS separations using a molecular modeling approach. J Chromatogr Sci. 2004; 42(7):383–387. [PubMed: 15355579]
47. Mendoza MC, Er EE, Blenis J. The Ras-ERK and PI3K-mTOR pathways: crosstalk and compensation. Trends Biochem Sci. 2011; 36(6):320–8. [PubMed: 21531565]
48. Zhang HH, Lipovsky AI, Dibble CC, Sahin M, Manning BD. S6K1 regulates GSK3 under conditions of mTOR-dependent feedback inhibition of Akt. Mol Cell. 2006; 24(2):185–97. [PubMed: 17052453]

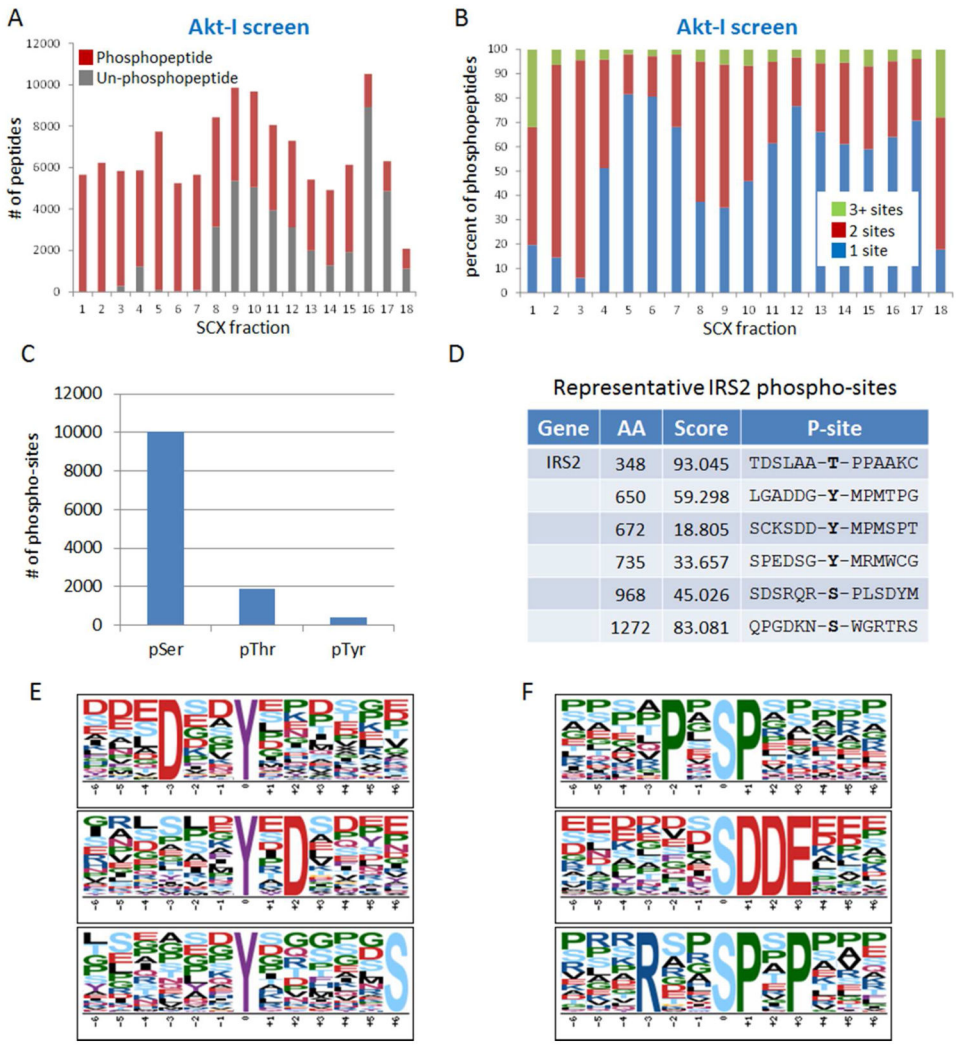

Figure 1.

Qualitative evaluation of the four ReDi phosphoproteomic analyses of insulin signaling in rat hepatocytes. (A) Number of phosphopeptides and unphosphopeptides identified from the 18 SCX fractions showing efficient phosphopeptide enrichment (data from the Akt-i screen). (B). Distribution of the phosphopeptides with 1, 2 or 3 phosphorylation sites in the 18 SCX fractions (data from the Akt-i screen). (C) Number of unique, and confidently localized phospho-serine (pSer), phospho-threonine (pThr) and phospho-tyrosine (p-Tyr) sites identified in the four ReDi screens. (D) Representative IRS2 phosphorylation sites identified from the four ReDi screens. (E) and (F) Representative phosphorylation motifs identified from the four ReDi screens on pTyr (E) and pSer (F), respectively.

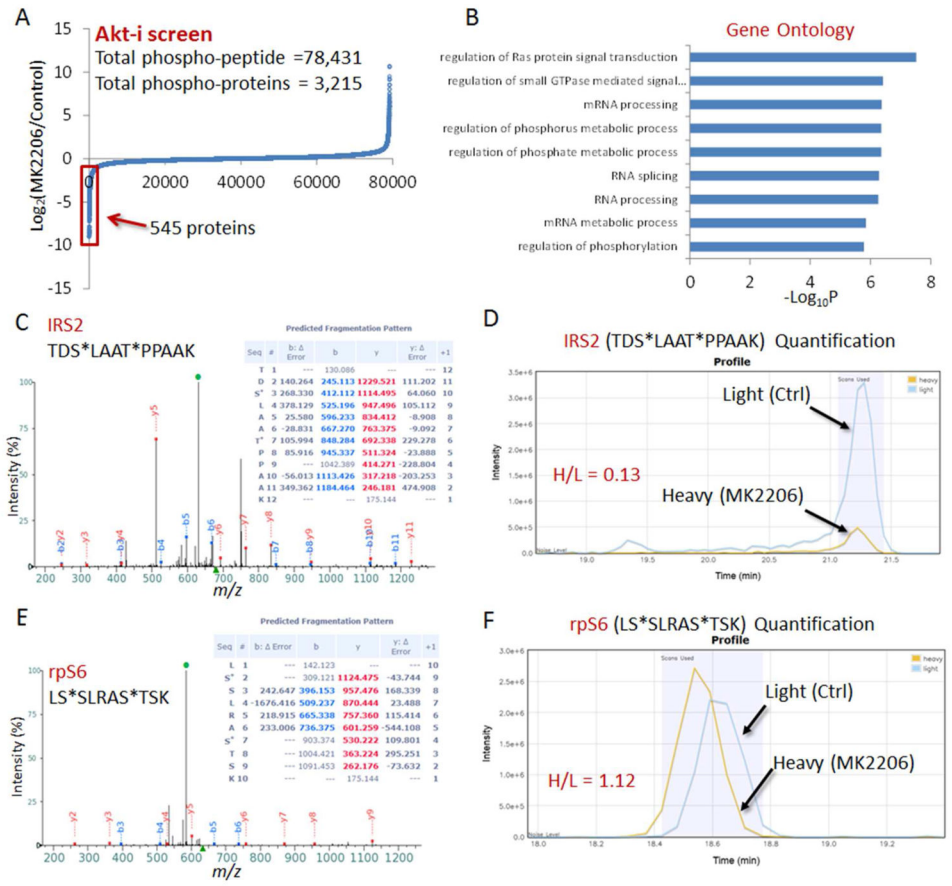

Figure 2.

Quantitative MS analysis of the Akt-regulated phosphoproteome in hepatocytes (Akt-i screen) (A) Distribution of Log_2 (Akt-i/control) of a total 78,431 phosphopeptides from 3,215 phospho-proteins showing that the vast majority of the peptides have equal amounts between MK2206-treated sample, and the control sample. Using a cutoff of 2-fold (phosphorylation decreased by 2-fold or more in MK2206-treated sample, compared to control), we identified 2033 phosphopeptides, which corresponded to 545 proteins. (B) Gene ontology analysis of the decreased proteins (proteins with decreased phosphorylation after MK2206 treatment) (C) Identification of an IRS2 phosphopeptide TDS*LAAT*PPAAK (the asterisks indicate that sites of phosphorylation). The green dot indicates the neutral loss peak. (D) The extracted ion chromatogram for the light and heavy version of the phosphopeptide as shown in (C). The abundance of the identified IRS2 phosphopeptide decreased by more than 7-fold after MK2206 treatment. L, light (insulin); H, heavy (insulin +MK2206). (E) Identification of a ribosomal protein S6 phosphopeptide LS*SLRAS*TSK (the asterisks indicate that sites of phosphorylation). The green dot indicates the neutral loss peak. (F) The extracted ion chromatogram for the light and heavy version of the phosphopeptide as shown in (E). The abundance of the identified ribosomal protein S6 phosphopeptide showed little change after MK2206 treatment. Note that there is a slight difference in the retention time profile between the light and heavy peptides, which is caused by the “deuterium effect”. In this case, it is important to integrate the peak area of the ion

chromatograms, rather than use maximal peak intensities, to accurately determine the heavy to light ratio. L, light (insulin); H, heavy (insulin+MK2206).

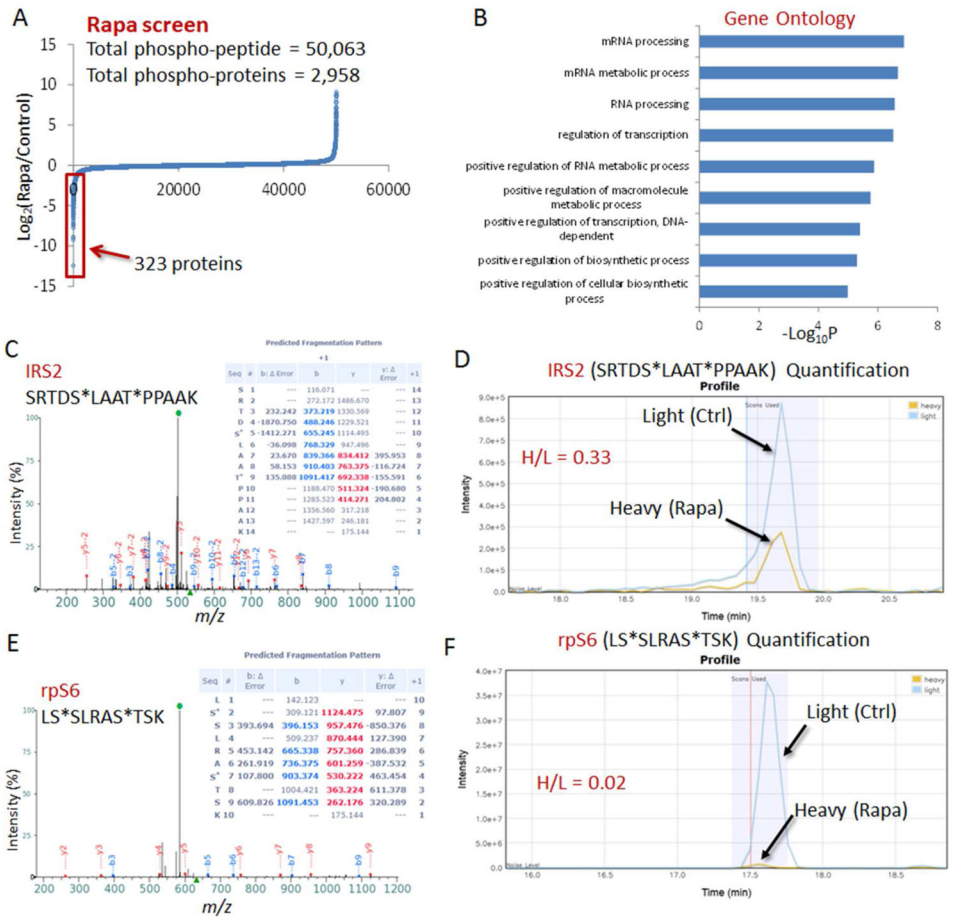

Figure 3.

Quantitative MS analysis of the mTORC1-regulated phosphoproteome in hepatocytes (Rapa screen) (A) Distribution of Log_2 (Rapamycin/Control) of a total 50,063 phosphopeptides from 2,958 phospho-proteins showing that the vast majority of the peptides have equal amounts between Rapamycin-treated sample, and the control sample. Using a cutoff of 2-fold (phosphorylation decreased by 2-fold or more in Rapamycin-treated sample, compared to control), we identified 954 phosphopeptides, which corresponded to 323 proteins. (B) Gene ontology analysis of the decreased proteins (proteins with decreased phosphorylation after Rapamycin treatment) (C) Identification of an IRS2 phosphopeptide SRTDS*LAAT*PPAAK (the asterisks indicate that sites of phosphorylation). The green dot indicates the neutral loss peak. (D) The extracted ion chromatogram for the light and heavy version of the phosphopeptide as shown in (C). The abundance of the identified IRS2 phosphopeptide decreased by more than 3-fold after Rapamycin treatment (E) Identification of a ribosomal protein S6 phosphopeptide LS*SLRAS*TSK (the asterisks indicate that sites of phosphorylation). The green dot indicates the neutral loss peak. (F) The extracted ion chromatogram for the light and heavy version of the phosphopeptide as shown in (E). The abundance of the identified ribosomal protein S6 phosphopeptide decreased by more than 50-fold after Rapamycin treatment.

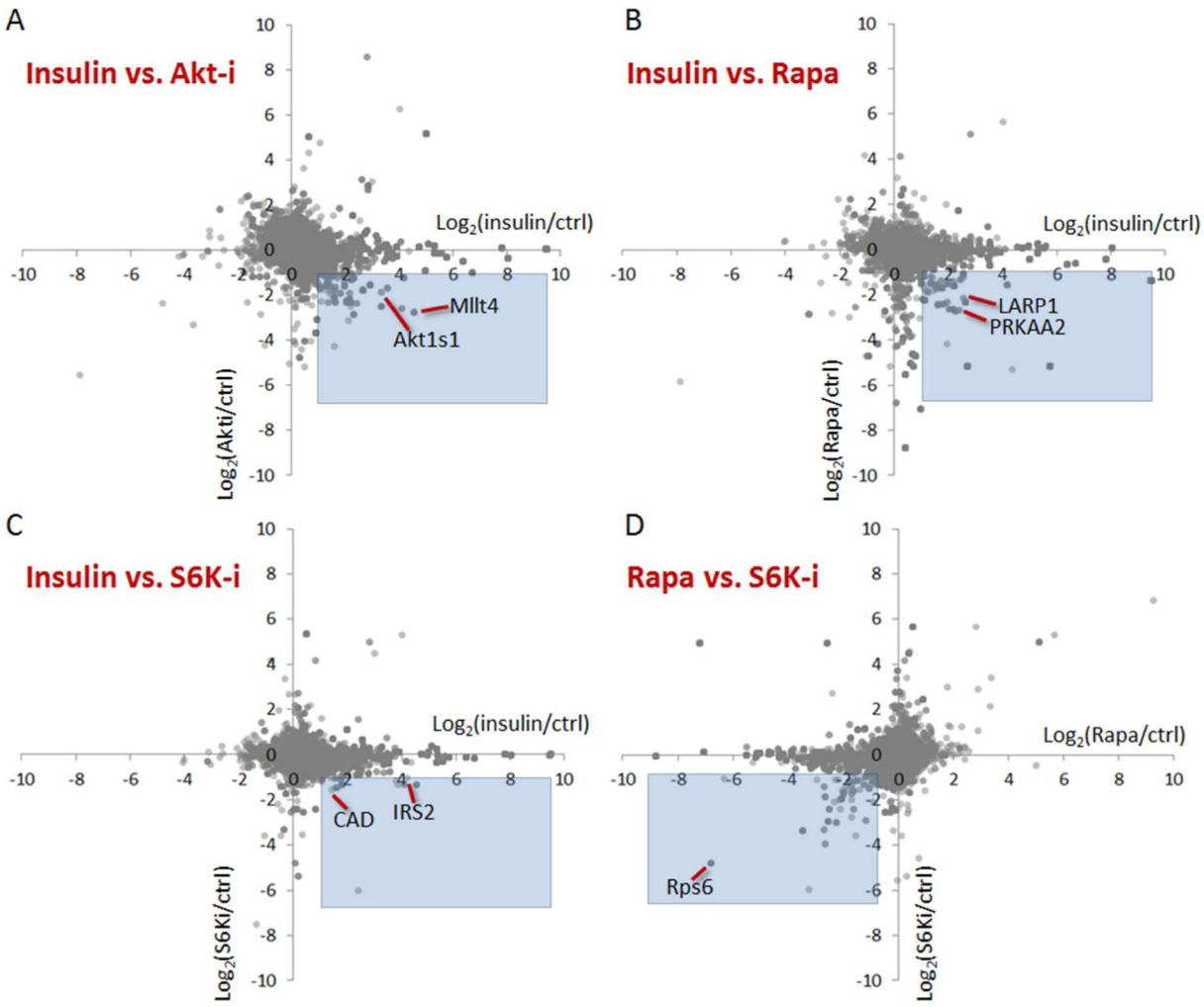

Figure 4.

Cross-reference analysis of the phosphoproteome regulated by key nodal kinases in the insulin signaling pathway in hepatocytes. The graph is a density plot, where the dark dots represent two or more overlapping phosphopeptides that have the same X,Y-values. The dots with light coloring represent one single phosphopeptide. (A) Cross-reference analysis of the insulin- vs. Akt-regulated phosphoproteome. Phosphopeptides commonly identified in the insulin screen and Akt-i screen (date from the 1st replicate experiment) were extracted, and their level of changes in their corresponding treatment conditions is plotted. The highlighted area represent peptides whose phosphorylation is increased by more 2-fold in the insulin screen, while is decreased by more than 2-fold in the Akt-i screen. (B) Cross-reference analysis of the insulin- vs. mTORC1-regulated phosphoproteome. Phosphopeptides commonly identified in the insulin screen and Rapa screen were extracted, and their level of changes in their corresponding treatment conditions is plotted. The highlighted area represent peptides whose phosphorylation is increased by more 2-fold in the insulin screen, while is decreased by more than 2-fold in the Rapa screen. (C) Cross-reference analysis of the insulin- vs. S6K-regulated phosphoproteome. Phosphopeptides commonly identified in the insulin screen and S6K-i screen were extracted, and their level of changes in their

corresponding treatment conditions is plotted. The highlighted area represent peptides whose phosphorylation is increased by more 2-fold in the insulin screen, while is decreased by more than 2-fold in the S6K-i screen. (D) Cross-reference analysis of the mTORC1- vs. S6K-regulated phosphoproteome. Phosphopeptides commonly identified in the Rapa screen and S6K-i screen were extracted, and their level of changes in their corresponding treatment conditions is plotted. The highlighted area represent peptides whose phosphorylation is decreased by more 2-fold in both the Rapa screen and S6K-i screen.

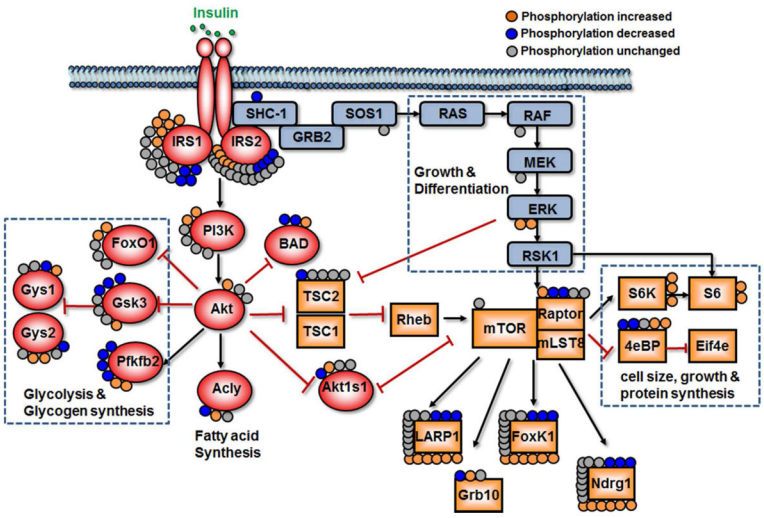

Figure 5.

Insulin-induced PI3K-Akt and MAPK network in hepatocytes. The pathway figure represents summarized literature-curated knowledge of the PI3K-Akt, MAPK and mTORC1 signaling networks. Phosphorylation sites are shown with colored circles: orange, increased by insulin; blue, decreased by insulin; gray, no change.